THE JOURNAL OF PHYSICAL CHEMISTRY LETTERS
A JOURNAL OF THE AMERICAN CHEMICAL SOCIETY

pubs.acs.org/JPCL

Letter

Recapture of the Nonvalence Excess Electron into the Excited Valence Orbital Leads to the Chemical Bond Cleavage in the Anion

Do Hyung Kang, Jinwoo Kim, and Sang Kyu Kim*

Cite This: J. Phys. Chem. Lett. 2021, 12, 6383−6388

Read Online

ACCESS | Metrics & More | Article Recommendations | Supporting Information

ABSTRACT: The excess electron in the dipole-bound state (DBS) of the anion is found to be recaptured into the excited valence orbital localized at the positive end of the dipole, leading to the chemical bond cleavage of the anion. In the DBS of the 4-iodophenoxide anion, the extremely loosely bound electron (binding energy of 53 cm^{-1}) is recaptured into the $\pi\sigma^*$ valence orbital, which is repulsive along the C−I bond extension coordinate, leading to the iodide (I^-) and phenoxyl diradical ($\cdot C_6H_4O\cdot$) channel at the asymptotic limit. This is the first real-time observation of the state-specific relaxation (other than autodetachment) dynamics of the DBS and subsequent chemical reaction. The lifetime of the 4-iodophenoxide DBS at its zero-point energy (ZPE), which is measured for the cryogenically cooled trapped anion using the picosecond laser pump−probe scheme, has been estimated to be ∼9.5 ± 0.3 ps. Quantum mechanical calculations support the efficient transition from the DBS (below the detachment threshold) to the low-lying $\pi\sigma^*$ valence orbital of the first excited state of the anion. Similar experiments on 4-chlorophenoxide and 4-bromophenoxide anions indicate that the electron recaptures into excited valence orbitals hardly occur in the DBS of those anions, giving the long lifetimes (≫ns) at ZPE, suggesting that the internal conversion to S_0 may be the major relaxation pathway for those anions.

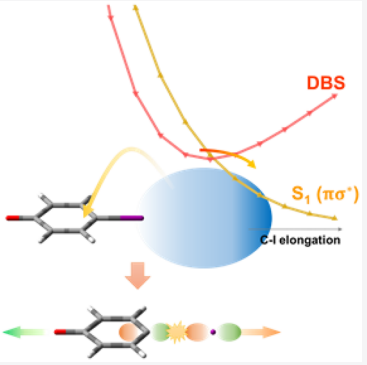

Electron attachment or detachment plays an important role as a gateway in electron transfer dynamics of many chemical or biological reactions including photosynthesis, aerobic respiration, or signaling of the fluorescent proteins.[1−3] Once the electron is transferred, the subsequent redox chemical reactions are strongly influenced by how the electron-driven energy relaxes into the molecular systems spatiotemporally, as it could be localized in specific areas or spread quickly over the entire body.[4] The relaxation dynamics following the electron attachment/detachment is therefore a very important issue to be resolved for thorough understanding of the entry/exit of electrons in the redox chemical reactions.[5,6] Relaxation of the electron-driven energy could also lead to the generation of the excited state of the anion species. It is quite rare to find a system where one can spectroscopically characterize the excited species of the anion. This is because the ultrafast direct/indirect detachment process (liberating the electron and radical) prevails quite often in the photoexcitation especially when the excited state is located near or above the electron-affinity (EA) threshold.[7,8] Therefore, photochemistry of the anion species still belongs to the uncharted field, although the anion chemistry has long been investigated extensively and intensively for many decades. The relaxation into the excited state of the anion thus could open a great opportunity for the investigation of the excited-state property of anionic species.

The dipole-bound state (DBS),[9−12] in which the electron is loosely bound to the radical moiety by a monopole−dipole long-range force, has been regarded as the nonvalence state of the anion species.[13−16] The electronically excited DBS is especially ubiquitous and has been known to play an important role as a "doorway state" in the formation of the interstellar anion species[17−19] or electron-mediated biological information transfer.[20−22] The DBS is metastable though, especially when its rovibrational states are above the detachment threshold, as it suffers the autodetachments via Feshbach resonances.[23,24] Although there have been a number of theoretical predictions[25,26] and experimental estimations[27−31] regarding autodetachment rates, the first direct measurement of the state-specific autodetachment rates of the DBS[32] (or quadruple-bound state[33]) was reported only quite recently by our group. On the other hand, the relaxation dynamics of the DBS at the (state-specific) molecular level has been little studied to date, although there have been a few femtosecond time-resolved studies identifying the dynamic role of the DBS in the relaxation processes in some interesting biological systems.[21,22,34,35] As the excess electron in the DBS is nonvalent in nature, understanding of the relaxation mechanism into the valence states is not straightforward. In this regard, the state-specific rate measurement of the DBS relaxation could be a

Received: June 5, 2021
Accepted: July 2, 2021
Published: July 7, 2021

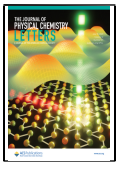

https://doi.org/10.1021/acs.jpclett.1c01789
J. Phys. Chem. Lett. 2021, 12, 6383−6388

valuable cornerstone for unravelling the otherwise formidable nonadiabatic coupling dynamics between nonvalence and valence orbitals.

Here, we report the real-time state-specific relaxation dynamics of the DBS of three different *para*-halogen atom substituted phenoxides (4-XPhO$^-$; X = Cl, Br, I) and the phenoxide (PhO$^-$). High-resolution spectroscopic study of the phenoxide (PhO$^-$) DBS was reported previously to give a binding energy of 97 cm^{-1}.[36,37] In 4-XPhO$^-$, the binding energy is decreased to 11, 24, or 53 cm^{-1} for 4-chlorophenoxide (4-ClPhO$^-$), 4-bromophenoxide (4-BrPhO$^-$), or 4-iodophenoxide (4-IPhO$^-$), respectively.[38] The decrease of the dipole moment upon the halogen atom substitution on the *para* position has been mainly attributed to the decrease of the DBS binding energy. In this work, we have investigated real-time dynamics of the DBS of those anions especially at their zero-point levels in order to isolate the sole relaxation dynamics only while minimizing other processes such as autodetachment. As the real-time relaxation dynamics of DBS has been first studied in a state-specific manner here, this work could be an important step forward for disentangling the dynamic role of the DBS as a doorway state to the valence-bound anions and subsequent chemical reactions.

Photodetachment spectra of PhO$^-$ and 4-XPhO$^-$ are obtained by monitoring the total photoelectron yield as a function of the picosecond laser wavelength ($\Delta\nu \approx 20$ cm^{-1}, $\Delta\tau \approx 1.7$ ps), Figure 1. In all spectra, the broad structureless background signal reflects ultrafast direct photodetachment. Sharp peaks on the top of the background then represent the Franck−Condon active DBS bands. All spectral features are consistent with the previous nanosecond spectra reported by the Wang group.[36−38] The zero-point levels of the DBS, which are located below the EA thresholds, could be clearly identified in PhO$^-$ and 4-IPhO$^-$, whereas those are hardly resolved in 4-ClPhO$^-$ and 4-BrPhO$^-$. Accordingly, the zero-point levels of these two latter DBS species are allocated based on the nanosecond photodetachment spectra in ref 38 in terms of the pump laser wavelength. For obtaining the transients, the pump wavelength is fixed to prepare the vibrational ground state of DBS, whereas the temporally delayed probe laser pulse (791 nm) has been employed to eject the electron. By monitoring the total photoelectron yield as a function of the pump−probe delay time, the DBS transient of each anion species could be obtained, Figure 2.

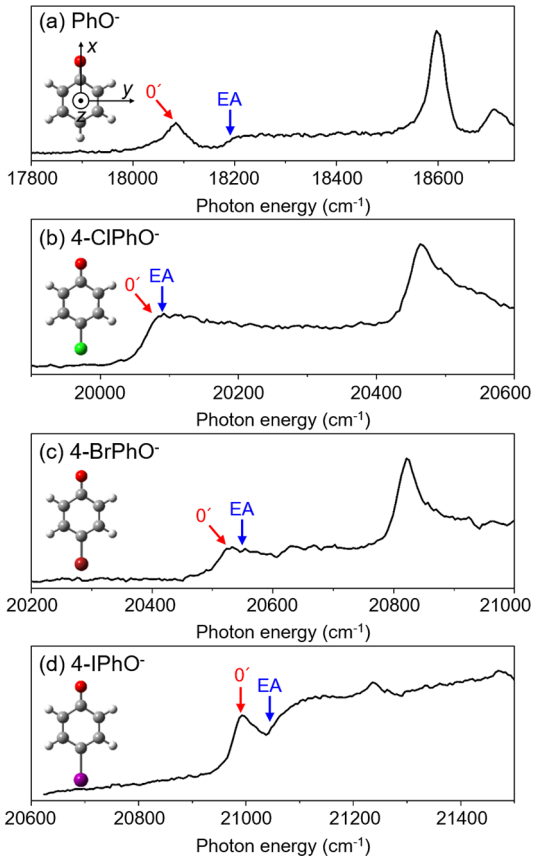

Figure 1. Photodetachment spectra of (a) PhO$^-$, (b) 4-ClPhO$^-$, (c) 4-BrPhO$^-$, and (d) 4-IPhO$^-$. The electron-affinity (EA) thresholds and the vibrational ground states of the dipole-bound state (DBS) are labeled in blue or red arrows, respectively. The geometry of the each anion and their Cartesian coordinates are shown in the inset.

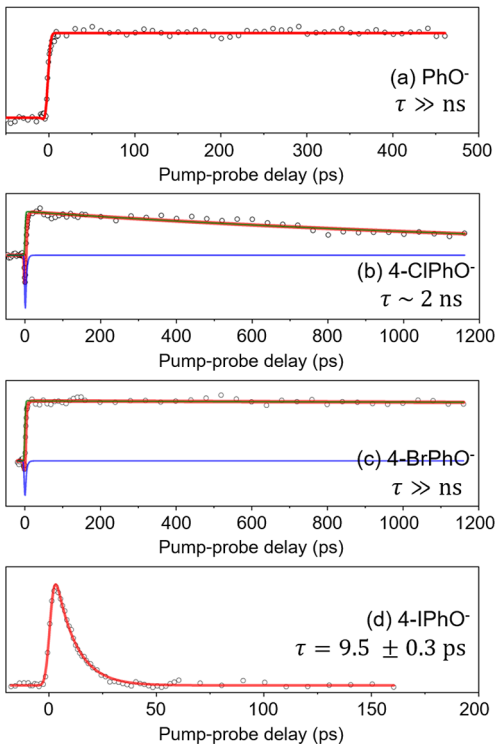

Figure 2. Picosecond total photoelectron transients taken on the vibrational ground state of DBS of (a) PhO$^-$, (b) 4-ClPhO$^-$, (c) 4-BrPhO$^-$, and (d) 4-IPhO$^-$. The transients of PhO$^-$ and 4-ClPhO$^-$ were fitted by a single-exponential decay function, while the transients of 4-ClPhO$^-$ and 4-BrPhO$^-$ were fitted by the biexponential decay function with opposite signs (see details in Supporting Information). Positive and negative decay functions are denoted in green and blue, respectively, whereas the entire fit function is denoted in red. The lifetimes of the positive decay components were extracted.

As reported earlier in ref 32, the PhO$^-$ transient shows no sign of temporal decay, indicating that the DBS at its ZPE survives for quite long. The DBS of 4-BrPhO$^-$ or 4-ClPhO$^-$ at their zero-point levels also shows very long lifetimes. Within our experimental time window of 1.2 ns, the DBS of the 4-BrPhO$^-$ does not show an even slight decay, indicating its lifetime could be much longer than tens of nanoseconds. For 4-ClPhO$^-$, however, the transient shows a definite decaying behavior with $\tau \approx 2$ ns for a partial component alongside the

https://doi.org/10.1021/acs.jpclett.1c01789
J. Phys. Chem. Lett. 2021, 12, 6383−6388

long-surviving component. These behaviors could be ascribed to the difference of two anions in their DBS binding energies. The DBS binding energy of the 4-BrPhO$^-$ is 24 cm^{-1}, which is much smaller than that of the and 4-IPhO$^-$ (53 cm^{-1}), whereas that of the 4-ClPhO$^-$ is even smaller to give 11 cm^{-1}.[38] As the spectral width of the picosecond pump laser is large (full width at half-maximum ≈ 20 cm^{-1}), it is quite plausible that the rotationally hot dipole-bound states above the EA threshold are partially populated in the pumping process especially for the 4-chlorophenoxide at the rotational temperature of 35 K (k_BT_{rot} ≈ 24 cm^{-1}).[33,39] Actually, in the canonical ensemble at 35 K, it is found that the percentage of the rotational ensemble exceeding the electron binding energy is estimated to be 0.4, 3.6, 15.4, or 34.7% for the DBS (ZPE) of PhO$^-$, 4-IPhO$^-$, 4-BrPhO$^-$, or 4-ClPhO$^-$, respectively (Supporting Information). Therefore, the slow decaying feature (τ ≈ 2 ns) observed in the 4-ClPhO$^-$ transient could be due to the autodetachment process of the rotationally hot species above the EA threshold. The significant population of the rotational ensemble above the EA threshold may also be partially responsible for the presence of the sharp depletion of the DBS transient at the time-zero, which is found only for two anions of 4-BrPhO$^-$ and 4-ClPhO$^-$ (*vide infra*). According to previous other studies on different molecular systems, the rotational autodetachment rate could be ranged from hundreds of ps to several ns, which is quite consistent with the present finding.[27−29]

The most remarkable finding in this work is that the DBS of the 4-IPhO$^-$ anion at the zero-point level, once populated, disappears completely with a lifetime (τ) of ∼9.5 ps. As the DBS at the zero-point level is below the EA threshold, the autodetachment channel is practically closed, and thus, its short lifetime should reflect the exceptionally fast nonradiative process. In order to unravel the DBS relaxation dynamics mechanism, we have calculated the vertical transition energies and orbitals of valence-bound excited states for each anion by the time-dependent density functional theory (TD-DFT). Interestingly, the singlet (S_1) of 4-IPhO$^-$ is calculated to be located just below the EA threshold, whereas that of PhO$^-$, 4-ClPhO$^-$, or 4-BrPhO$^-$ is predicted to be much higher than the detachment threshold, Figure 3. The S_1 state of 4-IPhO$^-$ has a characteristic of half-filling of the lowest-unoccupied molecular orbital (LUMO) and that of the highest-occupied molecular orbital (HOMO). While the HOMO represents the π orbital where the outmost electron is delocalized, the LUMO corresponds to the σ^* orbital, which is rather localized on the C−I bond moiety in a repulsive way. Relaxation of the DBS into the S_1 ($\pi\sigma^*$) state, therefore, should lead to C−I bond cleavage. This incidentally gives a very interesting perspective. Namely, one of two electrons in the π-HOMO of the ground (S_0) 4-IPhO$^-$ moves out to the loosely bound diffuse orbital in the DBS by photoexcitation. And then, the excess electron, which is remote from the radical core, is recaptured into the empty σ^*-LUMO in the relaxation process, leading to the C−I bond cleavage at the asymptotic limit. According to our TD-DFT, the vertical energetic difference between the D_0 and S_1 states is only ∼0.1 eV. Considering that the DBS is located just 53 cm^{-1} below D_0, it is most likely that the nonradiative transition from the DBS (at ZPE) to the S_1 state via the nonvalence to valence-state coupling is largely responsible for its short lifetime. It should be noted that the triplet (T_1: $\pi\sigma^*$) state is predicted to be located even below S_1 (Table 1). And yet, the intersystem crossing rate is expected to be much

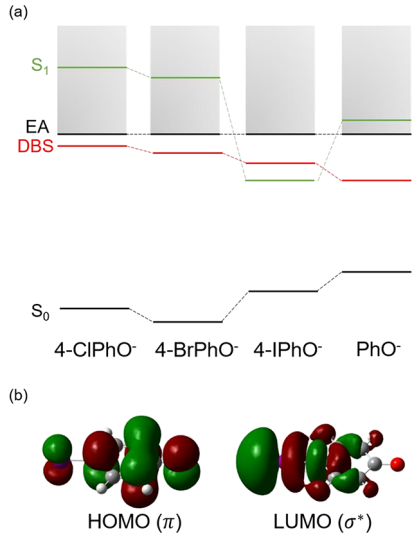

Figure 3. (a) Excited-state energy diagrams of the 4-ClPhO$^-$, 4-BrPhO$^-$, 4-IPhO$^-$, and PhO$^-$ calculated by the TD-DFT calculations. (b) Calculated HOMO and LUMO of the 4-IPhO$^-$. The S_1 state of 4-IPhO$^-$ corresponds to the transition from HOMO (π) to LUMO (σ^*).

slower compared to the internal conversion.[40] It is notable that the transition rate of (9.5 ps)$^{-1}$ is more or less similar to the previously reported other time-resolved results in terms of the order of magnitudes.[21,22,34,35] A subsequent chemical reaction could lead (diabatically) to the I$^-$ + PhO channel or (adiabatically) to the I + PhO$^-$ channel, where the only the former is thermodynamically plausible at the asymptotic limit, Figure 4. In the current experimental conditions, we could not detect I$^-$ as a final product. The C−I bond cleavage might take the (energetically inaccessible) adiabatic pathway with the higher probability. And yet, the finding and identification of the final products are subject to further investigation in the near future.

The relaxation pathway of the PhO$^-$, 4-BrPhO$^-$, or 4-ClPhO$^-$ DBS at its ZPE should include radiative and/or nonradiative transitions to S_0 and/or T_1. According to our TD-DFT calculations in Table 1, the DBS at ZPE of all those anions most likely relaxes into S_0, as no valence-bound excited states could be found below the EA threshold. It should be noted, however, that the contribution of the intersystem crossing to T_1 aided by the nuclear motions of certain vibrational modes cannot be completely excluded. For instance, although the TD-DFT calculation (B3LYP/6-311++G(d,p)) gives the T_1 ($\pi\sigma^*$) state of 4-BrPhO$^-$, which is located ∼0.05 eV above the EA threshold, the adiabatic potential of T_1 could be lowered along the C−Br elongation coordinate to allow the D_0/T_1 curve crossing mediated by the C−Br stretching motion. High-level *ab initio* calculations are highly desirable for thorough understanding of the complex relaxation dynamics of these interesting systems.

Time-resolved photoelectron imaging (TR-PEI) has been carried out for a better description of the photodetachment process, as it provides the two-dimensional picture of the photoelectron in both the energy and time domains (Supporting Information). In the TR-PEI spectra of 4-ClPhO$^-$ and 4-BrPhO$^-$, the photoelectron in the high-kinetic-energy region (0.3−1.6 eV) shows the biexponential decays, whereas the depletion (at the time-zero) followed by the exponential

https://doi.org/10.1021/acs.jpclett.1c01789
J. Phys. Chem. Lett. 2021, 12, 6383−6388

Table 1. Electron Affinities (EAs) and Valence-Bound Excited-State Energies of the PhO^- and 4-$XPhO^-$ Calculated by Using the B3LYP Level of Theory

	basis set	[a]EA (eV)	[b]EA (eV)	[c]exp (eV)	T_1 (eV)	S_1 (eV)
PhO^-	6-311++G(d,p)	2.21	2.27	2.25	2.43	2.43
4-$IPhO^-$	def2TZVP	2.44	2.50	2.61	2.11	2.42
4-$BrPhO^-$	6-311++G(3df,3pd)	2.49	2.56	2.55	2.60	2.81
4-$ClPhO^-$	6-311++G(d,p)	2.46	2.55	2.49	2.78	2.85

[a]Adiabatic EA. [b]Vertical EA. [c]Experimental values from refs 36 and 38.

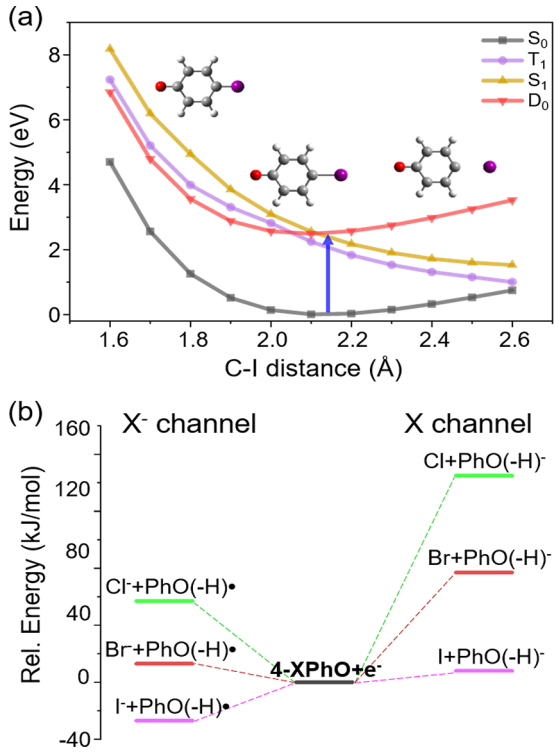

Figure 4. (a) Potential energy curves of S_0 (black), T_1 (purple), S_1 (yellow), and D_0 (red) of 4-$IPhO^-$ along the C−I elongation cooridate based on the TD-DFT calcuations (B3LYP/def2TZVP). Vertical transition from the ground-state optimized geometry is denoted as a blue arrow. (b) Thermodynamic energy diagrams of 4-$XPhO^-$ dissociation channels into the X^- or X product (green: 4-ClPhO, red: 4-BrPhO, and violet: 4-IPhO). The details of the calculation are depicted in the Supporting Information.

recovery have been observed for the photoelectron in the low-kinetic-energy range (0−0.1 eV). The time constant for the initial decay of the high-kinetic-energy electron ($\tau \approx 30$ or 45 ps for 4-$ClPhO^-$ or 4-$BrPhO^-$, respectively) matches with that estimated for the recovery of the low-kinetic-energy electron ($\tau \approx 40$ or 50 ps for 4-$ClPhO^-$ or 4-$BrPhO^-$, respectively) (Supporting Information). These transient patterns strongly indicate that the initial decay or recovery in the respective high- or low-kinetic-energy region is due to the autodetachment of the quantum states prepared above the EA threshold. It should be emphasized that the DBS at ZPE has not been well isolated for both 4-$ClPhO^-$ and 4-$BrPhO^-$, whereas it is clearly resolved for PhO^- or 4-$IPhO^-$, Figure 1. This suggests that the unidentified quantum states such as (ro)vibrationally excited states are most likely copopulated by the picosecond pump laser pulse in the preparation of the DBS of 4-$ClPhO^-$ and 4-$BrPhO^-$. This may also explain why the sharp depletion of the DBS transient at the time-zero is observed only for 4-$ClPhO^-$ and 4-$BrPhO^-$, Figure 2. Actually, the photoelectron image taken from the DBS of 4-$ClPhO^-$ at ZPE gives small peaks at the kinetic energies of ∼100 and 270 cm^{-1}, in addition to the Boltzmann-type distribution around the zero kinetic energy (Supporting Information). These peaks most likely result from the autodetachment through the two lowest-frequency vibrational modes of the 4-ClPhO radical, considering that their energies match very well with calculated ones of 108 (ν_{20}) and 274 (ν_{19}) cm^{-1}. Therefore, in the picosecond laser pumping process, the vibrationally hot bands (e.g., ν_{20}^1 or ν_{19}^1) seem to be coexcited. The autodetachment processes of such vibrationally excited states should be then reflected in the DBS transient. It should be noted, however, that it is not clear yet which quantum states are exactly involved in the optical pumping in the preparation of the DBS particularly at ZPE of 4-$ClPhO^-$ or 4-$BrPhO^-$, where the DBS origin is not clearly resolved in the present experimental condition. The temperature variation study would be highly desirable for identifying the origin of photoelectrons and associated transient behaviors.

Herein, we report the real-time observation of the relaxation dynamics of the DBS vibrational ground state in phenoxide and *para*-halogen substituted phenoxide anions using the picosecond pump−probe scheme employing time-resolved photoelectron imaging and cryogenically cooled ion-trap techniques. Especially, in the 4-iodophenoxide DBS, it has been found that the loosely bound excess electron (binding energy of 53 cm^{-1}) is recaptured into the $\pi\sigma^*$ valence orbital, which is repulsive along the C−I bond extension coordinate, leading to the iodide (I^-) and phenoxyl diradical ($\cdot C_6H_4O\cdot$) channel at the asymptotic limit. It is amazing to realize that the remote electron of the DBS is transferred to fill the empty σ^*-LUMO, leading to the eventual C−I bond cleavage reaction, opening a new type of anion excited-state chemistry. The TD-DFT calculations predict that the first excited state of the anion (S_1, $\pi\sigma^*$) is ∼0.1 eV lower than D_0 (radical), supporting the experimental finding that the 4-iodophenoxide DBS at the zero-point level survives only briefly with a lifetime of ∼9.5 ps. This is the first real-time state-specific observation of the nonradiative relaxation (and subsequent chemical reaction) mediated by the metastable DBS of the anion. The relaxation of the 4-chlorophenoxide or 4-bromophenoxide DBS at the zero-point level is found to be quite slow with a lifetime longer than tens of nanoseconds, indicating that the electron recaptures into excited valence orbitals hardly occur in the DBS of those anions. Rather, the internal conversion into the vibrationally hot S_0 state could be the main relaxation channel. The first real-time state-specific DBS relaxation dynamics in this work is expected to stimulate lots of experimental and theoretical challenges regarding the electron attachment/detachment dynamics as the role of the gateway in electron transfers in many important chemical and biological systems.

https://doi.org/10.1021/acs.jpclett.1c01789
J. Phys. Chem. Lett. 2021, 12, 6383−6388

EXPERIMENTAL METHODS

Details of the experimental apparatus have been described elsewhere.[33] Phenol or 4-XPhOH (1 mM, TCI Chemicals) was dissolved in a 9:1 methanol/water solvent mixture without further purifications in a 1 mM concentration. A few drops of ammonia solution were added to promote the deprotonation of the target neutral samples. The anions were sprayed by a homemade electrospray ionization (ESI) source, where a −3000 V voltage was applied and passed through a 180 °C heated capillary before being introduced into vacuum. The anions were then desolvated, accumulated by a dual-stage ion funnel (IF141, MassTech Inc.), and guided into the ion trap by a series of hexapole, quadrupole, and octopole ion guides (Ardara Technologies Inc.). Mass-selected anions were trapped and cooled in a cryogenic ion trap (8 K) with the aid of the 4:1 He/H_2 mixture buffer gas.[41] After the trapping time of ∼50 ms, the cryogenically cooled anions were extracted to the potential rereferencing tube,[42−44] guiding anions into the velocity map imaging (VMI) apparatus.[45−47] Photoelectrons ejected from anions were projected onto a two-dimensional position detector equipped with 40 mm diameter chevron-type microchannel plates (MCP, Photonis) backed by the P46 phosphor screen. Signals from the phosphor screen were recorded by a charge-coupled device (CCD) camera or photomultiplier tube (PMT). UV/vis picosecond laser pulses were generated from optical parametric amplifiers (OPAs, TOPAS-800, Light Conversion). The fundamental of the picosecond laser was produced from a picosecond Ti:Sapphire regenerative amplifier (Legend Elite-p, Coherent) combined with a femtosecond Ti:Sapphire oscillator (Vitara-T-HP, Coherent). Tunable UV/vis pulses were used as a pump pulse, while the fundamental output of the picosecond regenerative amplifier (791 nm) was used as a probe. The delay time between pump and probe pulses was scanned by an optical delay stage (DS220, Thorlabs) combined with retroreflectors (UBBR2.5-1UV, Newport).

ASSOCIATED CONTENT

Supporting Information

The Supporting Information is available free of charge at https://pubs.acs.org/doi/10.1021/acs.jpclett.1c01789.

Details of the time-resolved photoelectron imaging (TR-PEI) results, TD-DFT and thermodynamic calculations, and additional analysis for the rotational autodetachment (PDF)

AUTHOR INFORMATION

Corresponding Author

Sang Kyu Kim − *Department of Chemistry, KAIST, Daejeon 34141, Republic of Korea;* orcid.org/0000-0003-4803-1327; Email: sangkyukim@kaist.ac.kr

Authors

Do Hyung Kang − *Department of Chemistry, KAIST, Daejeon 34141, Republic of Korea;* orcid.org/0000-0003-4774-9062

Jinwoo Kim − *Department of Chemistry, KAIST, Daejeon 34141, Republic of Korea*

Complete contact information is available at: https://pubs.acs.org/10.1021/acs.jpclett.1c01789

Notes

The authors declare no competing financial interest.

ACKNOWLEDGMENTS

This work was supported by the National Research Foundation of Korea (2018R1A2B3004534, 2019K1A3A1A14064258, and 2019R1A6A1A10073887).

REFERENCES

(1) Lv, X.; Yu, Y.; Zhou, M.; Hu, C.; Gao, F.; Li, J.; Liu, X.; Deng, K.; Zheng, P.; Gong, W.; Xia, A.; Wang, J. Ultrafast Photoinduced Electron Transfer in Green Fluorescent Protein Bearing a Genetically Encoded Electron Acceptor. *J. Am. Chem. Soc.* **2015**, *137*, 7270−7273.

(2) Wang, H.; Lin, S.; Allen, J. P.; Williams, J. C.; Blankert, S.; Laser, C.; Woodbury, N. W. Protein Dynamics Control the Kinetics of Initial Electron Transfer in Photosynthesis. *Science* **2007**, *316*, 747−750.

(3) Gray, H. B.; Winkler, J. R. Electron Transfer in Proteins. *Annu. Rev. Biochem.* **1996**, *65*, 537−561.

(4) Benniston, A. C.; Harriman, A. Charge on the Move: How Electron-Transfer Dynamics Depend on Molecular Conformation. *Chem. Soc. Rev.* **2006**, *35*, 169−179.

(5) Hanel, G.; Gstir, B.; Denifl, S.; Scheier, P.; Probst, M.; Farizon, B.; Farizon, M.; Illenberger, E.; Märk, T. D. Electron Attachment to Uracil: Effective Destruction at Subexcitation Energies. *Phys. Rev. Lett.* **2003**, *90*, 188104.

(6) Horke, D. A.; Li, Q.; Blancafort, L.; Verlet, J. R. R. Ultrafast Above-Threshold Dynamics of the Radical Anion of a Prototypical Quinone Electron-Acceptor. *Nat. Chem.* **2013**, *5*, 711−717.

(7) Jagau, T.-C.; Bravaya, K. B.; Krylov, A. I. Extending Quantum Chemistry of Bound States to Electronic Resonances. *Annu. Rev. Phys. Chem.* **2017**, *68*, 525−553.

(8) Anstöter, C. S.; Bull, J. N.; Verlet, J. R. R. Ultrafast Dynamics of Temporary Anions Probed Through the Prism of Photodetachment. *Int. Rev. Phys. Chem.* **2016**, *35*, 509−538.

(9) Simons, J. Theoretical Study of Negative Molecular Ions. *Annu. Rev. Phys. Chem.* **2011**, *62*, 107−128.

(10) Jordan, K. D.; Wang, F. Theory of Dipole-Bound Anions. *Annu. Rev. Phys. Chem.* **2003**, *54*, 367−396.

(11) Lykke, K. R.; Mead, R. D.; Lineberger, W. C. Observation of Dipole-Bound States of Negative Ions. *Phys. Rev. Lett.* **1984**, *52*, 2221−2224.

(12) Fermi, E.; Teller, E. The Capture of Negative Mesotrons in Matter. *Phys. Rev.* **1947**, *72*, 399−408.

(13) Verlet, J. R. R.; Anstöter, C. S.; Bull, J. N.; Rogers, J. P. Role of Nonvalence States in the Ultrafast Dynamics of Isolated Anions. *J. Phys. Chem. A* **2020**, *124*, 3507−3519.

(14) Bull, J. N.; Verlet, J. R. R. Observation and Ultrafast Dynamics of a Nonvalence Correlation-Bound State of an Anion. *Sci. Adv.* **2017**, *3*, e1603106.

(15) Simons, J. Molecular Anions. *J. Phys. Chem. A* **2008**, *112*, 6401−6511.

(16) Compton, R. N.; Hammer, N. I. Multipole-bound Molecular Anions; *Advances in Gas Phase Chemistry*; Elsevier Science: New York, 2001; Vol. *4*, pp 257−305.

(17) Fortenberry, R. C.; Crawford, T. D. Theoretical prediction of new dipole-bound singlet states for anions of interstellar interest. *J. Chem. Phys.* **2011**, *134*, 154304.

(18) Mensa-Bonsu, G.; Lietard, A.; Tozer, D. J.; Verlet, J. R. R. Low energy electron impact resonances of anthracene probed by 2D photoelectron imaging of its radical anion. *J. Chem. Phys.* **2020**, *152*, 174303.

(19) Liu, G.; Ciborowski, S. M.; Graham, J. D.; Buytendyk, A. M.; Bowen, K. H. Photoelectron spectroscopic study of dipole-bound and valence-bound nitromethane anions formed by Rydberg electron transfer. *J. Chem. Phys.* **2020**, *153*, 044307.

(20) Burrow, P. D.; Gallup, G. A.; Scheer, A. M.; Denifl, S.; Ptasinska, S.; Märk, T.; Scheier, P. Vibrational Feshbach resonances in uracil and thymine. *J. Chem. Phys.* **2006**, *124*, 124310.
(21) Bull, J. N.; West, C. W.; Verlet, J. R. R. Ultrafast dynamics of formation and autodetachment of a dipole-bound state in an open-shell π-stacked dimer anion. *Chem. Sci.* **2016**, *7*, 5352−5361.
(22) Bull, J. N.; Anstöter, C. S.; Verlet, J. R. R. Ultrafast valence to non-valence excited state dynamics in a common anionic chromophore. *Nat. Commun.* **2019**, *10*, 5820.
(23) Tulej, M.; Güthe, F.; Pachkov, M. V.; Tikhomirov, K.; Xu, R.; Jungen, M.; Maier, J. P. Feshbach states of the propadienylidene anion H_2CCC^-. *Phys. Chem. Chem. Phys.* **2001**, *3*, 4674−4678.
(24) Zhu, G.-Z.; Wang, L.-S. High-resolution photoelectron imaging and resonant photoelectron spectroscopy via noncovalently bound excited states of cryogenically cooled anions. *Chem. Sci.* **2019**, *10*, 9409−9423.
(25) Acharya, P. K.; Kendall, R. A.; Simons, J. Vibration-induced electron detachment in molecular anions. *J. Am. Chem. Soc.* **1984**, *106*, 3402−3407.
(26) O'Neal, D.; Simons, J. Vibration-induced electron detachment in acetaldehyde enolate anion. *J. Phys. Chem.* **1989**, *93*, 58−61.
(27) Lykke, K. R.; Neumark, D. M.; Andersen, T.; Trapa, V. J.; Lineberger, W. C. Autodetachment spectroscopy and dynamics of CH_2CN^- and CD_2CN^-. *J. Chem. Phys.* **1987**, *87*, 6842−6853.
(28) Yokoyama, K.; Leach, G. W.; Kim, J. B.; Lineberger, W. C. Autodetachment spectroscopy and dynamics of dipole bound states of negative ions: $^2A_1-^2B_1$ transitions of H_2CCC^-. *J. Chem. Phys.* **1996**, *105*, 10696−10705.
(29) Yokoyama, K.; Leach, G. W.; Kim, J. B.; Lineberger, W. C.; Boldyrev, A. I.; Gutowski, M. Autodetachment spectroscopy and dynamics of vibrationally excited dipole-bound states of H_2CCC^-. *J. Chem. Phys.* **1996**, *105*, 10706−10718.
(30) Liu, H.-T.; Ning, C.-G.; Huang, D.-L.; Wang, L.-S. Vibrational Spectroscopy of the Dehydrogenated Uracil Radical by Autodetachment of Dipole-Bound Excited States of Cold Anions. *Angew. Chem., Int. Ed.* **2014**, *53*, 2464−2468.
(31) Albeck, Y.; Lunny, K. G.; Benitez, Y.; Shin, A. J.; Strasser, D.; Continetti, R. E. Resonance-Mediated Below-Threshold Delayed Photoemission and Non-Franck−Condon Photodissociation of Cold Oxyallyl Anions. *Angew. Chem., Int. Ed.* **2019**, *58*, 5312−5315.
(32) Kang, D. H.; An, S.; Kim, S. K. Real-Time Autodetachment Dynamics of Vibrational Feshbach Resonances in a Dipole-Bound State. *Phys. Rev. Lett.* **2020**, *125*, 093001.
(33) Kang, D. H.; Kim, J.; Cheng, M.; Kim, S. K. Mode-Specific Autodetachment Dynamics of an Excited Non-valence Quadrupole-Bound State. *J. Phys. Chem. Lett.* **2021**, *12*, 1947−1954.
(34) Yandell, M. A.; King, S. B.; Neumark, D. M. Time-Resolved Radiation Chemistry: Photoelectron Imaging of Transient Negative Ions of Nucleobases. *J. Am. Chem. Soc.* **2013**, *135*, 2128−2131.
(35) Kunin, A.; Neumark, D. M. Time-resolved radiation chemistry: femtosecond photoelectron spectroscopy of electron attachment and photodissociation dynamics in iodide−nucleobase clusters. *Phys. Chem. Chem. Phys.* **2019**, *21*, 7239−7255.
(36) Zhu, G.-Z.; Qian, C.-H.; Wang, L.-S. Dipole-bound excited states and resonant photoelectron imaging of phenoxide and thiophenoxide anions. *J. Chem. Phys.* **2018**, *149*, 164301.
(37) Liu, H.-T.; Ning, C.-G.; Huang, D.-L.; Dau, P. D.; Wang, L.-S. Observation of Mode-Specific Vibrational Autodetachment from Dipole-Bound States of Cold Anions. *Angew. Chem., Int. Ed.* **2013**, *52*, 8976−8979.
(38) Qian, C.-H.; Zhu, G.-Z.; Wang, L.-S. Probing the Critical Dipole Moment To Support Excited Dipole-Bound States in Valence-Bound Anions. *J. Phys. Chem. Lett.* **2019**, *10*, 6472−6477.
(39) Huang, D.-L.; Zhu, G.-Z.; Wang, L.-S. Communication: Observation of dipole-bound state and high-resolution photoelectron imaging of cold acetate anions. *J. Chem. Phys.* **2015**, *142*, 091103.
(40) Zhu, G.-Z.; Cheung, L. F.; Liu, Y.; Qian, C.-H.; Wang, L.-S. Resonant Two-Photon Photoelectron Imaging and Intersystem Crossing from Excited Dipole-Bound States of Cold Anions. *J. Phys. Chem. Lett.* **2019**, *10*, 4339−4344.
(41) Wang, X.-B.; Wang, L.-S. Development of a low-temperature photoelectron spectroscopy instrument using an electrospray ion source and a cryogenically controlled ion trap. *Rev. Sci. Instrum.* **2008**, *79*, 073108.
(42) Posey, L. A.; Johnson, M. A. Photochemistry of hydrated electron clusters $(H_2O)_n^-$ $(15 \leq n \leq 40)$ at 1064 nm: Size dependent competition between photofragmentation and photodetachment. *J. Chem. Phys.* **1988**, *89*, 4807−4814.
(43) Osterwalder, A.; Nee, M. J.; Zhou, J.; Neumark, D. M. High resolution photodetachment spectroscopy of negative ions via slow photoelectron imaging. *J. Chem. Phys.* **2004**, *121*, 6317−6322.
(44) McKay, A. R.; Sanz, M. E.; Mooney, C. R. S.; Minns, R. S.; Gill, E. M.; Fielding, H. H. Development of a new photoelectron spectroscopy instrument combining an electrospray ion source and photoelectron imaging. *Rev. Sci. Instrum.* **2010**, *81*, 123101.
(45) Chandler, D. W.; Houston, P. L. Two-dimensional imaging of state-selected photodissociation products detected by multiphoton ionization. *J. Chem. Phys.* **1987**, *87*, 1445−1447.
(46) Eppink, A. T. J. B.; Parker, D. H. Velocity map imaging of ions and electrons using electrostatic lenses: Application in photoelectron and photofragment ion imaging of molecular oxygen. *Rev. Sci. Instrum.* **1997**, *68*, 3477−3484.
(47) Parker, D. H.; Eppink, A. T. J. B. Photoelectron and photofragment velocity map imaging of state-selected molecular oxygen dissociation/ionization dynamics. *J. Chem. Phys.* **1997**, *107*, 2357−2362.

https://doi.org/10.1021/acs.jpclett.1c01789
J. Phys. Chem. Lett. 2021, 12, 6383−6388